Available online at www.sciencedirect.com

ScienceDirect

Energy Procedia 69 (2015) 879 – 890

Energy Procedia

International Conference on Concentrating Solar Power and Chemical Energy Systems, SolarPACES 2014

Object-oriented modeling of molten-salt-based thermocline thermal energy storage for the transient performance simulation of solar thermal power plants

I. Hernández Arriaga[a], F. Zaversky[b]*, D. Astrain[a]

[a]*Public University of Navarre (UPNA), Department of Mechanical, Thermal and Materials Engineering, Address: Campus Arrosadía s/n CP 31006, Pamplona, Spain*
[b]*National Renewable Energy Center (CENER), Solar Thermal Energy Department Address: c/ Ciudad de la Innovación 7, Sarriguren (Navarre), Spain*

Abstract

This paper presents a one-dimensional numerical model of a molten-salt-based thermocline thermal energy storage tank. The model is explained and referenced in detail, allowing for a complete reproduction. It has been successfully validated against experimental and theoretical data from the literature. Unlike previous works, the full boundary conditions of the performed validation simulations are given, enabling future model comparison studies and thus a further check for consistency against other codes. Finally, the model has been optimized regarding simulation speed for CSP performance simulations on system level.

Peer review by the scientific conference committee of SolarPACES 2014 under responsibility of PSE AG

Keywords: Concentrated solar power; thermal energy storage; thermocline; Modelica

1. Introduction

Solar thermal power, also known as concentrated solar power (CSP) or solar thermal electricity (STE) can be considered as a very promising technology when it comes to dispatchable and thus grid-friendly supply of renewable

* Corresponding author. Tel.: +34 625 234 628
E-mail address: fzaversky@cener.com, fritz.zaversky@alumni.tugraz.at

Peer review by the scientific conference committee of SolarPACES 2014 under responsibility of PSE AG
doi:10.1016/j.egypro.2015.03.116

electricity. This is due to the possibility of thermal energy storage (TES) that enables the decoupling between solar energy collection and electricity production. Additionally considering the fact that solar thermal power plants directly (the indirect usage of solar energy would be, e.g., the application of wind turbines) harness the abundant amount of solar energy incident on planet earth [1], they form a highly promising alternative to conventional fossil-fuel or nuclear technology, setting new standards in terms of environmental impact, sustainability and safety, and thus quality of life.

Nomenclature

CSP	concentrated solar power
DAE	differential-algebraic equation
MSL	Modelica Standard Library
TES	thermal energy storage
A_c	cross sectional area of the storage tank (m^2)
A_{fs}	surface area of solid fluid interface (m^2)
A_w	wall surface area (m^2)
c_f	specific heat capacity of fluid (J kg^{-1} K^{-1})
c_s	specific heat capacity of solid (J kg^{-1} K^{-1})
C_s	heat capacity of solid medium node (J/K)
d_p	particle diameter in packed bed (m)
$h_{fs\,nc}$	not corrected heat transfer coefficient between fluid and solid (W m^{-2} K^{-1})
h_{fs}	heat transfer coefficient between fluid and solid (W m^{-2} K^{-1})
k_f	thermal conductivity fluid (W m^{-1} K^{-1})
k_s	thermal conductivity solid (W m^{-1} K^{-1})
k_{fe}	effective thermal conductivity fluid (W m^{-1} K^{-1})
k_{se}	effective thermal conductivity solid (W m^{-1} K^{-1})
L	length of packed bed (m)
$\dot{m}_f$	fluid mass flow rate (kg/s)
M_f	mass of fluid (molten salt) per unit height of storage tank (kg/m)
M_s	mass of solid (packed-bed filling) per unit height of storage tank (kg/m)
n	number of nodes (integer)
P_{fs}	perimeter of fluid solid interface (m)
P_w	perimeter of wall fluid interface (m)
t	time (s)
T_a	ambient temperature (K)
T_f	fluid temperature (K)
T_s	solid temperature (K)
U	overall heat loss coefficient to ambient (W m^{-2} K^{-1})
v	flow velocity (m/s)
v_e	fluid velocity based on empty cross section (m/s)
x	coordinate along storage tank height (m)
Δp	pressure drop across packed bed (Pa)
ϵ	ratio of liquid phase volume to total volume - porosity (-)
μ_f	dynamic viscosity of fluid (Pa s)
ρ_f	density of fluid (kg m^{-3})
ρ_s	density of solid (kg m^{-3})

At today's commercial solar thermal power plants, the two-tank molten-salt-based sensible heat thermal energy storage system [2] is at the moment the state-of-the-art solution and is applied in indirect [3] (thermal-oil-based parabolic trough technology) or direct mode [4] (molten-salt-based central receiver technology). However, in order

to reduce costs a thermocline single-tank approach has been proposed by various authors. In this concept, the hot molten salt tank and the cold molten salt tank is replaced by just one tank containing the hot and the cold salt separated by a thermocline zone, i.e. a temperature gradient zone. A low-cost filler material (packed bed) should prevent convective mixing of the hot and the cold fluid, and furthermore, should provide the bulk of the thermal capacitance of the thermal energy storage [5]. Nevertheless, thermal ratcheting of the storage tank walls remains a significant design concern and further research is required in order to make the thermocline concept applicable at commercial level [6].

In order to assess the potential and operational aspects of the thermocline TES concept, modeling and simulation form crucial research and development activities. In principle, already presented models can be separated into 2 groups, namely (i) high-resolution three or two-dimensional numerical models suitable for a detailed thermal analysis (e.g. [7-9]), and (ii) one-dimensional numerical models of significantly lower spatial resolutions but thus suitable for computationally efficient transient performance simulations (e.g. [10-13]). Model group (ii) is typically based on slightly modified Schumann equations that were presented in their original form in a pioneering work [14] in 1929.

When thinking of system-level performance simulations of CSP plants, it is important to develop relatively simple but still accurate enough models enabling an efficient evaluation of the behavior of an entire solar thermal power plant. Therefore, Bayón & Rojas [15] recently proposed a simplified modeling method via fitting a logistic cumulative distribution function by using a validated numerical model of group (ii). In this way, it is possible to obtain the storage tank's outlet temperature as a function of time for both charging and discharging processes by a simple calculation. This represents a straightforward and valuable alternative to a numerical distributed parameter model that needs a certain minimum number of grid points and thus implies an increased computational effort in order to provide an acceptable accuracy.

Nevertheless, this work focuses on model category (ii), with the aim to discuss a non-causal proper physical model of a molten-salt-based thermocline TES tank. In particular, a well-structured and flexible model is presented, giving also importance to a simulation-platform-independent implementation, thus maximizing the reusability and exchangeability of the developed code.

2. The methodology and the modeling approach

Given the importance and already widespread usage of Modelica [16] as an interdisciplinary and extremely flexible modeling language, it has also been applied for this work's modeling procedure. Modelica is a multi-purpose physical system modeling language and has been developed in an international effort in order to unify already existing similar modeling approaches and to enable developed models and model libraries to be easily exchanged. The concept is based on non-causal models featuring true ordinary differential and algebraic equations, i.e. differential-algebraic equation (DAE) systems [16].

2.1. The modified Schumann equations used in this work

In the following, the governing partial differential equations of a one-dimensional thermocline packed-bed TES system will be stated. Subsequently, their discretization, implementation and numerical integration will be explained in detail.

$$M_f c_f \frac{\partial T_f}{\partial t} + M_f c_f v \frac{\partial T_f}{\partial x} = h_{fs} P_{fs} \left(T_s - T_f\right) + k_{fe} A_c \frac{\partial^2 T_f}{\partial x^2} - U P_w \left(T_f - T_a\right) \quad (1)$$

$$M_s c_s \frac{\partial T_s}{\partial t} = h_{fs} P_{fs} \left(T_f - T_s\right) + k_{se} A_c \frac{\partial^2 T_s}{\partial x^2} \quad (2)$$

where

$$M_f = \epsilon A_c \rho_f \quad (3)$$

$$M_s = (1-\epsilon)\, A_c\, \rho_s \tag{4}$$

$$v = \frac{\dot{m}_f}{\rho_f\, \epsilon\, A_c} \tag{5}$$

The above set of coupled partial differential equations (PDEs) has to be discretized in order to obtain a set of ordinary differential equations (ODEs) suitable for the model formulation in Modelica. This has been done according to the finite volume method (FVM). In particular, the developed model is based on well-proven and freely available model structures and base classes, as provided by the Modelica Standard Library (MSL) [17].

2.2. The 1-D finite volume approach according to the MSL and the implementation of the thermocline flow model

The MSL offers a rigorous implementation of a one-dimensional fluid flow model according to the finite volume method [18], which forms the basis of the thermocline flow model developed in this work. Basically, the total flow volume is discretized in n finite control volumes along the flow direction. In order to avoid a multiple definition of the basic mass and energy balances, the one-dimensional thermocline flow model extends from the MSL base class "partial distributed volume". This generic base class defines the mass and energy balances in terms of net mass flow, net enthalpy flow, net heat flow $\dot{Q}_{net}$ and net work flow $\dot{W}_{net}$, for each control volume i (see Fig. 1). This can be written as follows:

$$m_i = V_i \cdot \rho_i \tag{6}$$

$$\frac{dm_i}{dt} = \dot{m}_{a,\,i} - \dot{m}_{b,\,i} \tag{7}$$

$$U_i = m_i \cdot u_i \tag{8}$$

$$\frac{dU_i}{dt} = \dot{m}_{a,\,i} \cdot h_{a,\,i} - \dot{m}_{b,\,i} \cdot h_{b,\,i} + \dot{Q}_{net,\,i} + \dot{W}_{net,\,i} \tag{9}$$

Note: for a positive mass flow at the right control volume boundary ($\dot{m}_{b,\,i} > 0$, see Fig. 1), $h_{b,\,i}$ is the specific enthalpy leaving the control volume, which corresponds to the specific enthalpy h_i of the control volume i; for $\dot{m}_{b,\,i} < 0$, $h_{b,\,i}$ is the specific enthalpy h_{i+1} of the corresponding adjacent control volume upstream; for $\dot{m}_{a,\,i} > 0$, $h_{a,\,i}$ is the specific enthalpy h_{i-1} of the corresponding adjacent control volume upstream; for $\dot{m}_{a,\,i} < 0$, $h_{a,\,i}$ is the specific enthalpy h_i of the control volume i; the net work flows $\dot{W}_{net,\,i}$ are set to zero in this work.

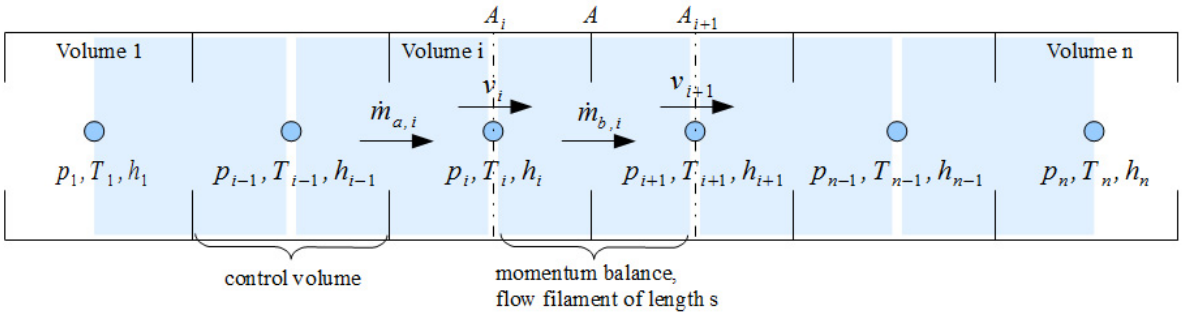

Fig. 1. Finite volume discretization scheme according to the staggered grid approach [19]

In order to correctly implement Eq. (1), the net heat flow term $\dot{Q}_{net}$ of each control volume (in Eq. (9)) has to be defined correspondingly. According to Eq. (1), the net heat flow $\dot{Q}_{net}$ of each control volume depends on three

factors, namely (i) on the convective heat transfer from the fluid to the solid phase (or vice versa), (ii) on the heat transfer via axial conduction in the liquid phase, and (iii) on the heat loss to the ambient:

$$\dot{Q}_{net} = \dot{Q}_{convective} + \dot{Q}_{net\ conductive} - \dot{Q}_{heat\ loss} \quad (10)$$

2.2.1. The forced convective heat transfer model

The forced convective heat transfer model has been implemented as a replaceable sub-model, similar to the corresponding wall heat transfer model in a simple tube model as explained in Ref. [20]. Basically, this model calculates the heat flow between the fluid and the solid via estimating the fluid-to-solid heat transfer coefficient h_{fs} using a Nusselt number correlation as published by Alazmi & Vafai [21]:

$$Nu = \frac{h_{fs\,nc}\, d_p}{k_f} = 2 + 1.1\, Re^{0.6}\, Pr^{1/3} \quad (11)$$

Additionally, since the particles are considered as lumped capacities at uniform temperature (see Section 2.3), the final heat transfer coefficient is obtained via a dimensionless correction factor that is a function of the Biot number as given in Eq. (7) of Ref. [22]. This defines the forced convective heat flow between the solid and the fluid as follows:

$$\dot{Q}_{convective} = \frac{h_{fs\,nc}}{1+\frac{Bi}{5}}\, A_{fs}\left(T_s - T_f\right) = h_{fs}\, A_{fs}\left(T_s - T_f\right) \quad (12)$$

2.2.2. The model of the axial conduction within the fluid

Like the convective heat transfer, also the axial conduction has been implemented in a specific sub-model class that is then instantiated within the thermocline flow model. This axial conduction model calculates the net heat flow for each control volume due to axial conduction according to a staggered grid approach, i.e. it calculates the heat flows between the temperature nodes defined by the thermodynamic states (shaded dots in Fig. 1) within each control volume and determines then the final net heat flow for each volume via the difference between entering and leaving conductive flows. For instance, the heat flow $\dot{Q}_{conductive}$ between volume *i* and *i+1* is calculated according to the following equation:

$$\dot{Q}_{conductive} = \frac{k_{fe,i} + k_{fe,i+1}}{2}\, \frac{A_c}{\Delta x}\left(T_{f,i} - T_{f,i+1}\right) \quad (13)$$

where k_{fe} is defined according to Ref. [21] as follows:

$$k_{fe} = \epsilon\, k_f \quad (14)$$

2.2.3. The model of the heat loss to the ambient

The model of the heat loss to the ambient has been implemented according to a quasi-steady approach considering an overall heat transfer coefficient U. This defines the heat flow to the ambient per control volume as follows:

$$\dot{Q}_{heat\ loss} = UA_w\left(T_f - T_a\right) \quad (15)$$

It has to be noted that only considering the heat loss between the fluid and the ambient is a simplification of the actual problem (since, strictly speaking, also the solid medium is in contact with the tank's wall), especially at offline mode of the storage system where the mass flow is set to zero and the heat transfer between the fluid and the solid is not dominated by convection. Nevertheless, this simplification has shown to be acceptable when validating the model against experimental data provided by Pacheco et al. [5].

2.2.4. The pressure drop model

The pressure drop across a packed bed may be calculated according to the following correlation as published by Ergun [23]:

$$\frac{\Delta p}{L} = 150\frac{(1-\epsilon)^2}{\epsilon^3}\frac{\mu_f v_e}{d_p^2} + 1.75\frac{1-\epsilon}{\epsilon^3}\frac{\rho_f v_e^2}{d_p} \quad (16)$$

2.3. The 1-D model of the packed bed – A distributed lumped capacitance approach

Having formulated all the necessary equations for describing the fluid flow within the thermocline thermal energy storage system, the solid medium (the packed bed) inside the storage tank has to be defined in order to complete the model. This has been done according to a distributed lumped capacitance approach, i.e. the solid filling is discretized in sections along the flow assigning one representative temperature variable to each of the discrete sections and lumping the solid mass per discrete section in this temperature node.

The thermal conduction within the solid material is considered in the same way as for the fluid, i.e. applying Eq. (13) correspondingly for the solid material, obtaining the heat flows between two neighboring nodes as follows:

$$\dot{Q}_{conductive,\ s} = \frac{k_{se,i} + k_{se,i+1}}{2}\frac{A_c}{\Delta x}\left(T_{s,i} - T_{s,i+1}\right) \quad (17)$$

where k_{se} is defined according to Ref. [21] as follows:

$$k_{se} = (1-\epsilon)\,k_s \quad (18)$$

In order to connect the model of the solid medium to the fluid flow model, i.e. to the convective heat transfer sub-model, a Modelica heat connector (red squares in Fig. 2) is added to each node of the distributed lumped capacitance model. Thus, the governing equation for one of the n solid material nodes can be formulated as follows, using $\dot{Q}_{convective}$ from Eq. (12):

$$C_s \cdot \frac{dT_s}{dt} = \dot{Q}_{net\ conductive,\ s} - \dot{Q}_{convective} \quad (19)$$

2.4. Media properties

Within the MSL, all specific media property functions are decoupled from the library components by defining a replaceable "medium package" in each of them. Basically, all fluid property function names and interfaces are defined within the base class "partial medium". In order to allow for a full replaceability, each specific medium model extends from this base class the "partial medium" and defines the specific medium related relationships by redeclaring each necessary medium property function. Thus, every single component of the library that covers the modeling of fluid is not limited to a single specific medium. In fact, it can easily be adapted for the use of different media, by simply replacing the default medium package when instantiating the final model.

In this work, two different media models for molten salts are used. For the model validation, a model for Hitec XL has been implemented according to Siegel et al. [24]. For the subsequent application of the model, the commonly applied solar salt (60% $NaNO_3$ and 40% KNO_3) has been considered using property equations as given by Zavoico [25].

The solid media properties have been implemented similarly, also providing a replaceable solid medium model for the filler material. In this case, the solid medium properties have been implemented independent of temperature according to Xu et al. [9] for quartzite rock.

2.5. The final molten-salt-based thermocline thermal energy storage model

The final comprehensive Modelica class of the thermocline thermal energy storage system consists of the thermocline flow model as described in Section 2.2 and the model of the solid medium as described in Section 2.3. When instantiating the model, the fluid medium model and the solid medium model are re-declared according to the specific modeling needs. Fig. 2 displays the model scheme.

2.6. The model's translation and its numerical integration, i.e. simulation

The developed Modelica code has been translated into numerical simulation code using a state-of-the-art commercial Modelica tool, applying its differential-algebraic system solver DASSL [26, 27]. This algorithm applies an implicit method for the numerical integration of the governing ordinary differential equations. In particular, it approximates the derivatives using a k^{th} order backward differentiation formula, where k ranges from 1 to 5. At every step it chooses the order and the step size based on the behavior of the solution. Newton's method is used to solve the resulting equations for the solutions at each discrete point in time [26, 27].

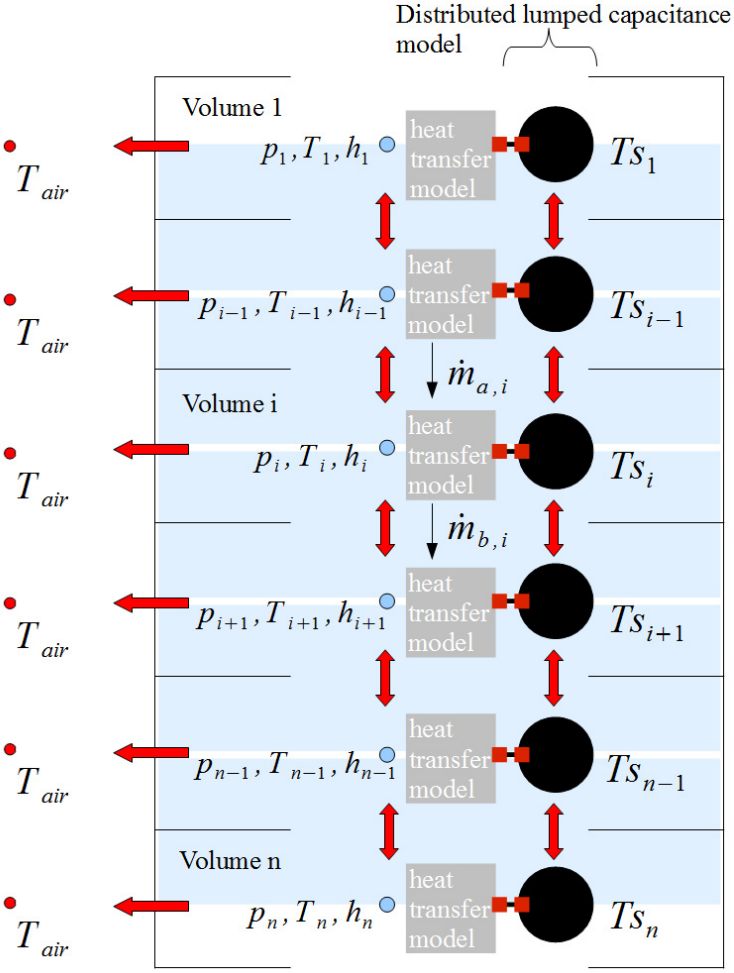

Fig. 2. Thermocline TES model scheme

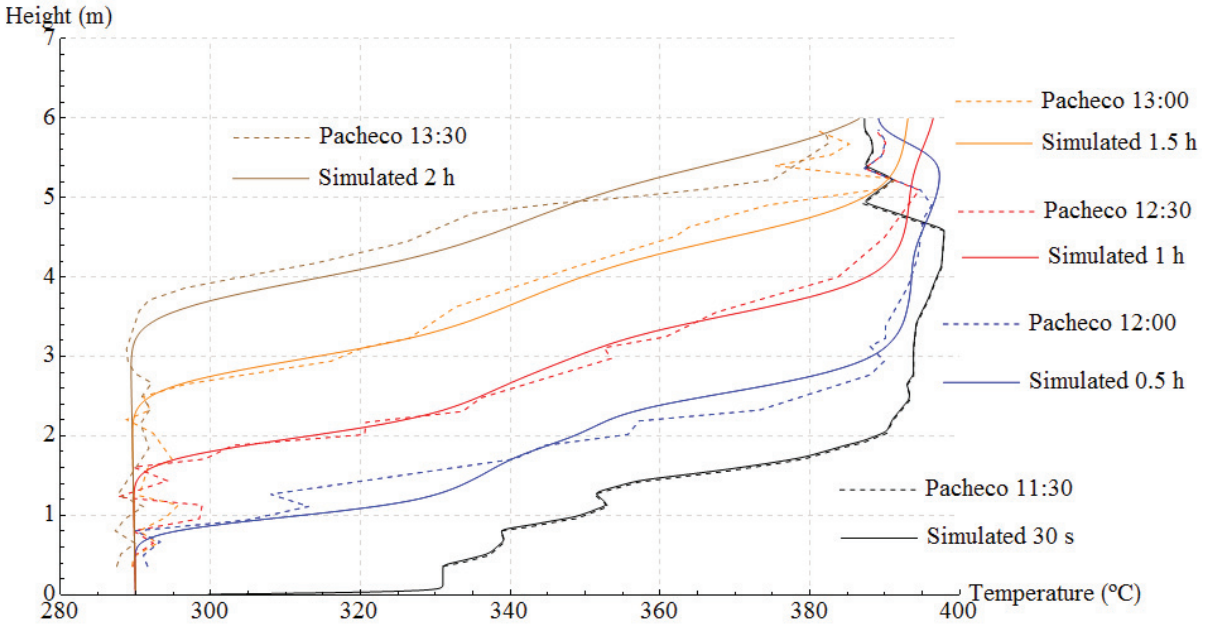

Fig. 3. Thermocline TES model experimental validation against data from Ref. [5]

3. The experimental and theoretical model validation

In order to check the simulation results for consistency, they have been compared to experimental data available in the open literature. In particular, the well-known experiments performed by Pacheco et al. [5] have been considered. Thus, the model's geometry parameters have been set accordingly (tank height: 6 m, tank diameter: 3 m, particle diameter: 0.01905 m, porosity: 0.22). Furthermore, the overall heat loss coefficient U has been set to 0.757 W m^{-2} K^{-1}, a typical value when assuming a mineral wool insulation layer thickness of 14 cm [28]. Finally, the initial temperature distribution within the tank has been set to the one as given in Fig. 8 of Ref. [5] at time 11:30, assuming the solid and the liquid phase in thermal equilibrium at each node at simulation start. However, unfortunately, the mass flow rate entering the storage tank at the bottom, an important boundary condition of this discharge experiment, is not stated in Ref. [5]. Only a rough number of the total thermal energy extracted is given, which only allows an approximate calculation of the mean mass flow rate during the presented experiment. For this reason, some iterative simulations have been performed varying the mass flow rate of the molten salt nearby the approximated value in order to fit the simulation results best with the experimental data. In this way, best results have been obtained with a constant mass flow rate of 6 kg/s throughout the 2 hours experiment. The results are shown in Fig. 3 (solid lines). It can be said, that the movement of the thermocline zone upwards is captured quite well. It should be noted that the chosen number n of control volumes has been set to 600, clearly showing grid independence for the simulation results.

Additionally, the model's results have also been compared to simulation data presented by Xu et al. [29]. In particular, the effective discharge times of the simulations as presented in Fig. 6 (a) of Ref. [29] have been considered. Table 1 shows the values obtained by Xu et al. [29] as well as the values obtained by this work's model. It can be observed that the results correlate quite well at realistic particle diameters (small Biot numbers) where the lumped capacitance approach forms a valid simplification of the real heat transfer problem.

Table 1. Comparison of effective discharge times (outlet temperature > 370 ºC)

Particle diameter (m)	Effective discharge time Xu et al. [29] (*h*)	Effective discharge time of this work's model (*h*)
0.01	4.632	4.767
0.019	4.607	4.683
0.05	4.474	4.4
0.1	4.214	4.017
0.25	3.436	3.083

4. The up-scaling of the experimental setup to 1010 MWh of thermal capacity and model optimization

This section will deal with the up-scaling of the experimental-scale model setup in order to obtain a full-size thermocline thermal energy storage tank that could be used at a typical 50 MWe parabolic trough collector power plant featuring about 1010 MWh of thermal energy storage capacity. In summary, the full-size dimensions of the thermocline tank can be estimated by a straightforward thermal calculus, considering the heat capacity of the solid filler material and the heat capacity of the molten salt as well as the applied temperature difference, which gives a storage tank diameter of about 43 m when assuming a tank height of 12 m and applying solar salt as storage fluid.

However, the determination of the required spatial resolution of the model is somewhat challenging, since a good trade-off between model accuracy and simulation speed has to be found. This especially holds for system-level simulations of solar thermal power plants, where it is important to optimize long-term performance models regarding their complexity and hence computational intensity [30].

Basically, the higher the chosen number of control volumes or nodes is, the closer is the numerical solution to the real behavior, typically converging to the true solution of the governing partial differential equations in a certain number-of-nodes interval, i.e. when increasing the number of control volumes above a certain given threshold, the increase in model accuracy is negligible small, making models of higher spatial resolution generally useless.

Thus, in order to give recommendations for suitable levels of discretization, a typical discharge simulation has been performed multiple times varying the chosen number of nodes n. It has been observed that the simulation results converge around 1200 nodes, i.e. at a spatial resolution of about 0.01 m (volumes height). Fig. 4 plots the relative error in effective discharge time and effective discharge efficiency (see Eq. (20) of Ref. [9]) over the number of control volumes, based on the model having 1200 control volumes. It can be observed that by reducing the number of control volumes to 100 (instead of applying 1200, where the results converge), the introduced relative error in simulation results constitutes about 5%. Taking the notable increase in simulation speed into account (a 10 hours experiment requires only 16 seconds of simulation time on a standard desktop computer, instead of roughly one hour as for the case of 1200 nodes), a spatial resolution of about 12 cm (12 m / 100 nodes) represents a good trade-off for simulations on system level. Due to inherent modeling uncertainties, for example when thinking of the application of empirical Nusselt number correlations for the forced convective heat transfer, one gets hardly ever closer to the real behavior than within ±5%.

Additionally, it has been observed that the optimum spatial resolution depends on the modeled storage tank height. The higher the storage tank is, the lower is the required spatial resolution in order to obtain the same relative error in simulation results, based on the reference model where results converge. Fig. 5 displays the relationships between relative error (based on the reference models where results converge) and control volume height for storage tank setups featuring total heights of 6, 12 and 18 m. Basically, this behavior may be explained by the fact that larger tank heights lead to higher maximum thermocline thicknesses [31], which means that the temperature gradient zone expands over a larger height interval of the tank requiring a lower spatial resolution for the same level in numerical relative error. Obviously, since it is only a one-dimensional model, the relative error of simulation results does not depend on the chosen diameter of the thermocline storage tanks (see the two cases in Fig. 5 having the same total tank height, 12 m, but different tank diameters, 43 and 3 m – here the evolution of the relative error is practically the same).

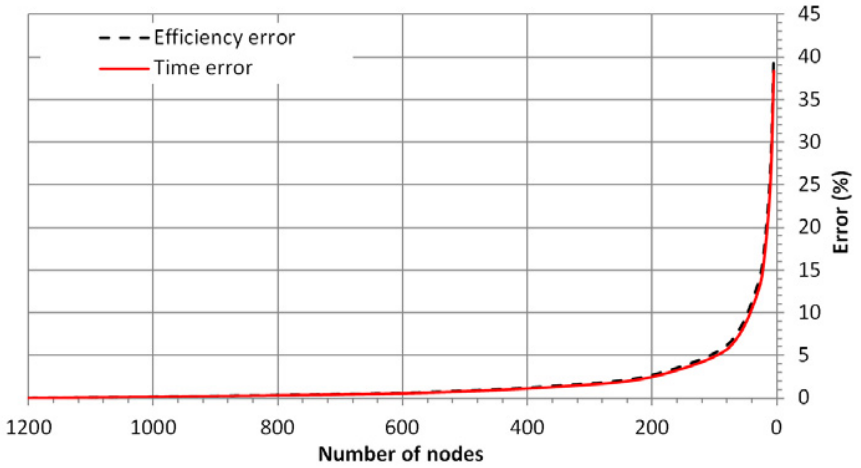

Fig. 4. Effective discharge time and efficiency relative error

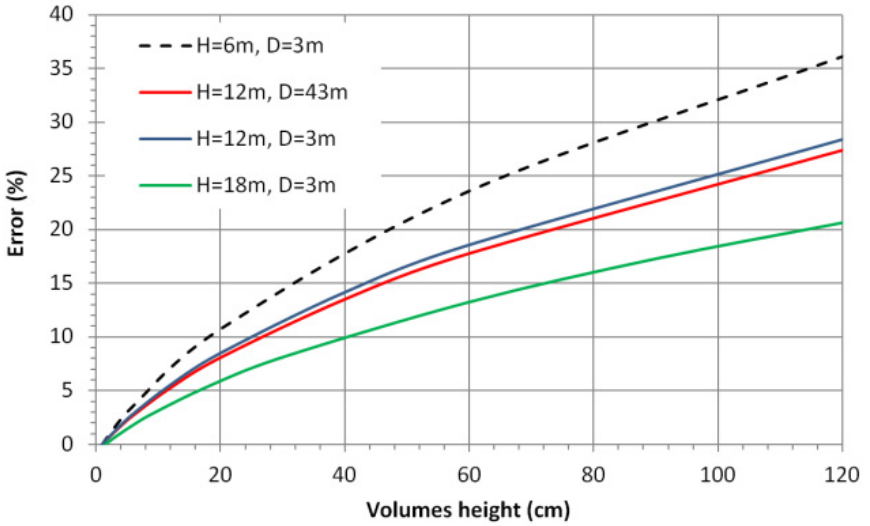

Fig. 5. Model relative error vs. height of control volumes

5. Conclusions and outlook

This work presents the development and the application of a one-dimensional model of a molten-salt-based thermocline thermal energy storage tank. The modeling procedure builds upon a thorough literature review and emphasis has been given on a simulation-platform-independent implementation of the thermocline TES model, in particular, applying Modelica as modeling language. The numerical model has been successfully validated against experimental and numerical data available in open literature.

Subsequently, the model has been up-scaled from the experimental-scale setup, to represent a full-size thermocline TES tank, having a capacity of about 1010 MWh, thus being equivalent to TES system dimensions of current commercial projects. After performing a grid-independence test, i.e. after determining the number of control volumes where the simulation results converge, the model has been optimized for simulation speed (which is important for CSP performance simulations on system level) of course accepting a certain small error when compared to the reference setup.

For the specific case having a storage tank height of 12 m, it has been shown that a choice of 100 control volumes, equally distributed along the height of the tank, leads to relative errors of about 5% when compared to the model setup where numerical results converge (1200 control volumes). Considering the notable rise in calculation speed, this spatial resolution of 12 cm should be seen as a typical default setting for the thermocline model component within a solar thermal power plant model library, which of course has to be adapted for the specific simulation to be performed.

The presented model forms a valuable basis for solar thermal power plant performance simulations on system level. The task of future works is clearly the model's application in a comprehensive transient performance model of a CSP plant, being able to establish, improve and optimize operation as well as control strategies for future solar thermal power plants that apply the thermocline thermal energy storage concept.

References

[1] D. Abbott, Keeping the energy debate clean: How do we supply the world's energy needs?, Proceedings of the IEEE, 98 (2010) 42-66.
[2] U. Herrmann, B. Kelly, H. Price, Two-tank molten salt storage for parabolic trough solar power plants, Energy, 29 (2004) 883-893.
[3] S. Relloso, E. Delgado, Experience with Molten Salt Thermal Storage in a Commercial Parabolic Trough Plant. Andasol-1 Commissioning and Operation, SolarPACES, Berlin, Germany 2009.
[4] S. Relloso, J. Lata, Molten Salt Thermal Storage: A Proven Solution to Increase Plant Dispatchability. Experience in Gemasolar Tower Plant, SolarPACES, Granada, Spain, 2011.
[5] J.E. Pacheco, S.K. Showalter, W.J. Kolb, Development of a molten-salt thermocline thermal storage system for parabolic trough plants, Journal of Solar Energy Engineering, 124 (2002) 153-159.
[6] S. Flueckiger, Z. Yang, S.V. Garimella, Review of molten-salt thermocline tank modeling for solar thermal energy storage, Heat Transfer Engineering, 34 (2013) 787-800.
[7] Z. Yang, S.V. Garimella, Thermal analysis of solar thermal energy storage in a molten-salt thermocline, Solar Energy, 84 (2010) 974-985.
[8] S. Flueckiger, Z. Yang, S.V. Garimella, An integrated thermal and mechanical investigation of molten-salt thermocline energy storage, Applied Energy, 88 (2011) 2098-2105.
[9] C. Xu, Z. Wang, Y. He, X. Li, F. Bai, Sensitivity analysis of the numerical study on the thermal performance of a packed-bed molten salt thermocline thermal storage system, Applied Energy, 92 (2012) 65-75.
[10] A.C. McMahan, Design and Optimization of Organic Rankine Cycle Solar-Thermal Powerplants, Master's Thesis, University of Wisconsin-Madison, USA, 2006.
[11] J.T. Van Lew, P. Li, C.L. Chan, W. Karaki, J. Stephens, Transient heat delivery and storage process in a thermocline heat storage system, ASME 2009 International Mechanical Congress and Exposition IMECE 2009, Lake Buena Vista, Florida, USA, 2009.
[12] S.M. Flueckiger, B.D. Iverson, S.V. Garimella, J.E. Pacheco, System-level simulation of a solar power tower plant with thermocline thermal energy storage, Applied Energy, 113 (2014) 86-96.
[13] A. Modi, C.D. Pérez-Segarra, Thermocline thermal storage systems for concentrated solar power plants: One-dimensional numerical model and comparative analysis, Solar Energy, 100 (2014) 84-93.
[14] T.E.W. Schumann, Heat transfer: A liquid flowing through a porous prism, Journal of the Franklin Institute, 208 (1929) 405-416.
[15] R. Bayón, E. Rojas, Analytical function describing the behaviour of a thermocline storage tank: A requirement for annual simulations of solar thermal power plants, International Journal of Heat and Mass Transfer, 68 (2014) 641-648.
[16] H. Elmqvist, S.E. Mattsson, Modelica - The next generation modeling language - An international design effort, Proceedings of the 1st World Congress on System Simulation, Singapore, 1997.
[17] Modelica-Association, Modelica Standard Library 3.2 - Free library from the Modelica Association to model mechanical (1D/3D), electrical (analog, digital, machines), thermal, fluid, control systems and hierarchical state machines, Modelica-Association, http://www.modelica.org (accessed 14.11.2012), 2010.
[18] R. Franke, F. Casella, M. Sielemann, K. Proelss, M. Otter, M. Wetter, Standardization of Thermo-Fluid Modeling in Modelica.Fluid Proceedings 7th Modelica Conference, Como, Italy, 2009.
[19] H. Tummescheit, Design and Implementation of Object-Oriented Model Libraries using Modelica, PhD Thesis Department of Automatic Control - Lund Institute of Technology, Lund, Sweden, 2002.
[20] F. Zaversky, M. Sánchez, D. Astrain, Object-oriented modeling for the transient response simulation of multi-pass shell-and-tube heat exchangers as applied in active indirect thermal energy storage systems for concentrated solar power, Energy, 65 (2014) 647-664.
[21] B. Alazmi, K. Vafai, Analysis of Variants Within the Porous Media Transport Models, Journal of Heat Transfer, 122 (2000) 303-326.
[22] C.P. Jeffreson, Prediction of breakthrough curves in packed beds: I. Applicability of single parameter models, AIChE Journal, 18 (1972) 409-416.
[23] S. Ergun, Fluid flow through packed columns, Chemical Engineering Progress, 48 (1952) 89-94.
[24] N.P. Siegel, R.W. Bradshaw, J.B. Cordaro, A.M. Kruizenga, Thermophysical property measurement of nitrate salt heat transfer fluids, ASME 5th International Conference on Energy Sustainability, Washington, DC, USA, 2011.
[25] A.B. Zavoico, Solar Power Tower Design Basis Document - Revision 0, Sandia National Laboratories, Albuquerque, New Mexico 87185 and Livermore, California 94550, 2001.

[26] L.R. Petzold, A description of DASSL: A differential/algebraic system solver, Sandia National Laboratories, Albuquerque, New Mexico, USA, 1982.
[27] K.E. Brenan, S.L. Campbell, L.R. Petzold, Numerical Solution of Initial-Value Problems in Differential-Algebraic Equations, SIAM - Society for Industrial and Applied Mathematics, Philadelphia, USA, 1996.
[28] I. Hernández-Arriaga, Desarollo de modelos de simulación para sistemas de almacenamiento térmico en termoclina para centrales solares - MSc Thesis, Public University of Navarre, Pamplona, Spain, 2014.
[29] C. Xu, X. Li, Z. Wang, Y. He, F. Bai, Effects of solid particle properties on the thermal performance of a packed-bed molten-salt thermocline thermal storage system, Applied Thermal Engineering, 57 (2013) 69-80.
[30] F. Zaversky, Object-oriented modeling for the transient performance simulation of solar thermal power plants using parabolic trough collectors - A review and proposal of modeling approaches for thermal energy storage, PhD Thesis, Public University of Navarre, Pamplona, Spain, 2014.
[31] C. Xu, Z. Wang, Y. He, X. Li, F. Bai, Parametric study and standby behavior of a packed-bed molten salt thermocline thermal storage system, Renewable Energy, 48 (2012) 1-9.